

<https://doi.org/10.1038/s41698-025-00936-3>

# Multi-cancer detection of circulating tumor cells by targeting oncofetal chondroitin sulfate

Check for updates

Caroline Løppke<sup>1</sup>, Randi Ugleholdt<sup>2,3</sup>, Christine F. Secher<sup>4</sup>, Nicolai T. Sand<sup>5</sup>, Joana Mujollari<sup>1</sup>, Tobias Gustavsson<sup>1</sup>, Robert Dagil<sup>1</sup>, Thor G. Theander<sup>1</sup>, Ali Salanti<sup>1</sup>, Kristoffer S. Rohrberg<sup>2,4</sup> & Mette Ø. Agerbæk<sup>1,5</sup>✉

Liquid biopsies for the detection of circulating tumor cells (CTCs) are a promising strategy for personalized cancer management. However, traditional CTC detection platforms are often constrained to epithelial cancers, vulnerable to phenotypic changes, and rely on specialized devices for standardized detection, restricting the clinical utility across diverse cancer types and healthcare settings. In this study, we present a tumor-agnostic, platform-independent CTC detection strategy based on recognition of the cancer-specific glycosylation, oncofetal chondroitin sulfate (ofCS). Through coupling of the ofCS-binding protein, VAR2CSA, to a fluorophore-carrying dextran polymer, we successfully detected ofCS-positive CTCs from blood samples in two diverse and independent cohorts comprising early- and late-stage cancer patients of both epithelial and non-epithelial tumor origin. In addition, no ofCS-positive cells were detected in non-malignant controls. Thus, targeting of ofCS has the potential to expand the range of patients who could benefit from CTC analysis, enhancing the clinical utility in various cancer settings.

The release of tumor-derived products into the blood circulation provides an easy accessible source for the molecular characterization of cancers, enabling diagnosis, prognostic stratification, and ability to monitor treatment efficacy<sup>1</sup>. Circulating tumor cells (CTCs) are one of the most studied liquid analytes as these cells cause the dissemination of cancers and contain phenotypic and genotypic information about the tumor<sup>2</sup>. Although CTCs hold great promise as cancer biomarkers, the rarity of these tumor cells in the blood along with their heterogenic nature, pose considerable challenges toward routine clinical implementation<sup>3,4</sup>.

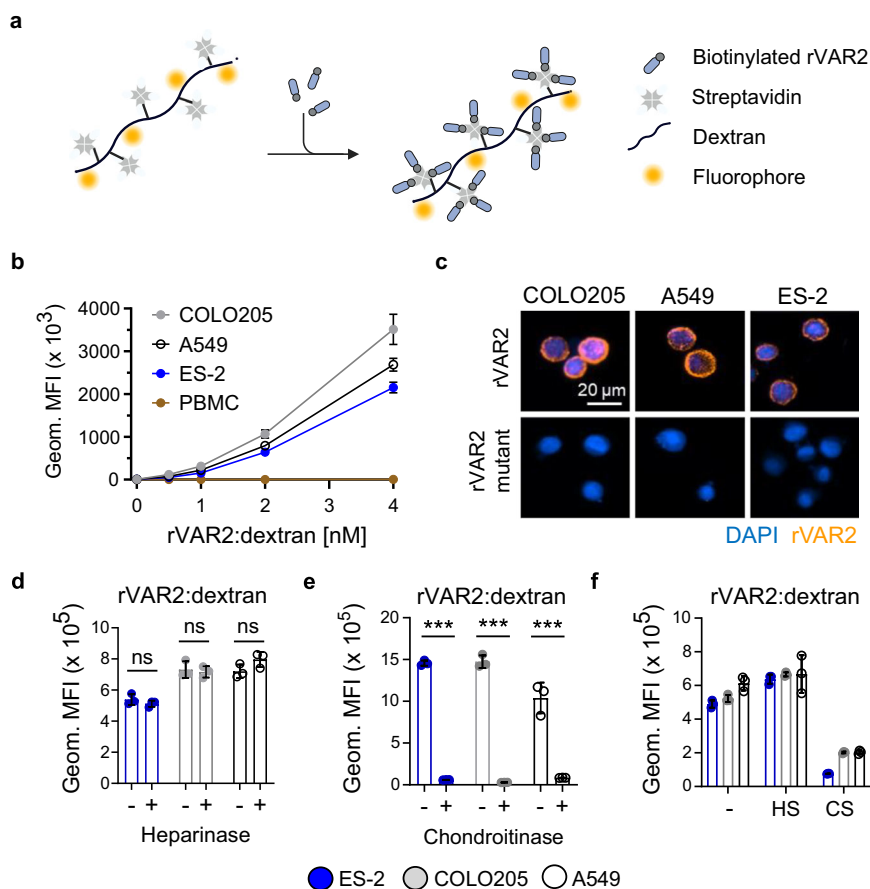
Strategies for enrichment of CTCs from a blood sample can essentially be divided into antigen-dependent and antigen-independent methods, exploiting distinct phenotypic traits or physical characteristics of the CTCs. So far, antigen-dependent methods have primarily been applied to patients with epithelial cancers by utilizing antibodies against the epithelial cellular adhesion molecule (EpCAM) not expressed on leukocytes for magnetic retrieval followed by cancer-specific detection using pan-cytokeratin (CK) antibodies<sup>5–7</sup>. However, the use of antibodies towards one or few epithelial proteins

renders CTC detection vulnerable to changes in expression level or downregulation of the selected marker<sup>8–10</sup>. Alternatively, strategies based on depletion of leukocytes<sup>11</sup> or antigen-independent separation of CTCs from healthy blood cells based on biophysical properties such as cell size, deformability, electrical charge, and density<sup>5,12</sup>, have improved isolation of CTCs of non-epithelial origin or low expression of epithelial markers. Yet, as most epitope-independent platforms co-isolate varying levels of white blood cells along with cancer cells, these still benefit from downstream detection, which can be difficult due to lack of specific mesenchymal markers. Therefore, new markers that are unaffected by cancer origin and phenotypic changes, such as those occurring during epithelial to mesenchymal transition (EMT), are needed to improve detection of a broad repertoire of CTCs.

Compelling evidence links tumorigenesis with fetal development with shared features that include cell differentiation, proliferation, migration, and a high degree of immune evasion<sup>13,14</sup>. In cancer, fetal-like reprogramming of malignant cells involves re-expression of oncofetal proteins or glycosylations normally silenced in healthy adult tissues<sup>15,16</sup>. Although various

<sup>1</sup>Centre for translational Medicine and Parasitology at Department of Immunology and Microbiology, Faculty of Health and Medical Sciences, University of Copenhagen and Department of Infectious Disease, Copenhagen University Hospital, 2200 Copenhagen, Denmark. <sup>2</sup>Department of Clinical Medicine, Faculty of Health and Medical Sciences, University of Copenhagen, Copenhagen, Denmark. <sup>3</sup>Department of Medicine, Copenhagen University Hospital – Herlev and Gentofte, Herlev, Denmark. <sup>4</sup>Department of Oncology, Copenhagen University Hospital, Rigshospitalet, Denmark. <sup>5</sup>VarCT Diagnostics, 2000 Frederiksberg, Denmark. ✉e-mail: [mettea@sund.ku.dk](mailto:mettea@sund.ku.dk)

**Fig. 1 | rVAR2:dextran binds CS on cancer cells with high specificity.** **a** Graphic representation of the rVAR2:dextran staining strategy. **b** Binding of PE-labelled rVAR2:dextran to three cancer cell lines (ES-2, COLO205, A549) and PBMCs from a healthy donor as measured by flow cytometry (mean and SD of triplicate measurements). **c** Staining of the cancer cell lines with 4 nM of biotinylated rVAR2 or rVAR2 mutant (DBL1-ID2a<sup>555</sup>AAAAIAAA<sup>562</sup>) coupled to the PE-labelled dextran backbone (orange). The cell nuclei were counterstained with DAPI (blue). **d, e** Binding of PE-labelled rVAR2:dextran to the cancer cell lines with or without pre-treatment with Heparinase (2.5 mU/mL Heparinase II + 5 mU/mL Heparinase III) or Chondroitinase ABC (20 µg/mL) as measured by flow cytometry (mean and SD of triplicate measurements). P-value were determined by one-way ANOVA, ns = non-significant, \*\*\*p < 0.001. **f** Binding of PE-labelled rVAR2:dextran to the cancer cell lines with or without competition with 25 µg/mL soluble heparan sulfate (HS) or soluble chondroitin sulfate (CS). Graph shows mean and SD of triplicate measurements.



oncofetal plasma proteins such as alpha-fetoprotein or carcinoembryonic antigen (CEA) are used as biomarkers routinely in clinical settings, limited attention has been given to oncofetal markers as a strategy for CTC detection<sup>17,18</sup>. We have previously shown that a distinct type of glycosaminoglycan termed oncofetal chondroitin sulfate (ofCS) is abundant in both placental and malignant tissues<sup>16,19</sup>. Structurally, ofCS is assembled from repeating disaccharide units, and makes up long unbranched carbohydrate chains that can be modified by sulfations at various positions<sup>20</sup>. Importantly, a multitude of proteins at the cancer cell surface can be post-translationally modified with ofCS chains, securing a broad ofCS display independent of changes in expression of single proteins<sup>21</sup>. Thus, surface-bound ofCS on CTCs may serve as a robust cancer marker compared to traditional surface proteins. We have previously shown that a recombinant version of the malaria parasite protein VAR2CSA (rVAR2) specifically binds ofCS in a wide range of malignancies with limited binding to noncancerous tissues except the placenta<sup>16</sup>. Since this discovery, the unique cancer-specific binding of rVAR2 has been explored within cancer diagnostics with a focus on using the protein as a capture agent for magnetic isolation of CTCs<sup>22–24</sup>. This strategy has allowed isolation of CTCs from glioma, pancreatic, hepatic, and prostate cancer patients, demonstrating the utility of ofCS as a cancer marker in both epithelial and mesenchymal cancers<sup>22,24,25</sup>. In extension of this work, we hypothesized that rVAR2 could be used for direct detection of CTCs in blood, thereby bypassing the need for magnetic enrichment or size-based separation technologies. For this purpose, we developed a platform-independent approach for CTC detection based on the staining of all nucleated cells from a blood sample using rVAR2 coupled to a fluorophore-labeled dextran. In this study, we demonstrate the feasibility of the staining workflow in a diverse set of clinical blood samples from patients with non-specific symptoms and signs of cancer referred to a diagnostic outpatient clinic as well as in a cohort of patients with advanced cancer.

## Results

### rVAR2 bound to a dextran backbone binds ofCS on the cancer cells

Directly modifying rVAR2 with fluorophores can affect the specificity and affinity of the interaction with ofCS. Instead, we coupled biotinylated rVAR2 to a dextran backbone (rVAR2:dextran) carrying multiple streptavidin molecules and PE-fluorophores, which resulted in a higher avidity of the rVAR2 protein combined with an enhanced fluorescence signal as illustrated in Fig. 1a. To test if the cancer specificity of rVAR2 was preserved after dextran coupling, we evaluated the binding of the rVAR2:dextran by flow cytometry on three different cancer cell lines from lung (A549), ovarian (ES-2) and colorectal cancer (COLO205), as well as on healthy human peripheral blood mononuclear cells (PBMCs). All three cancer cell lines bound rVAR2:dextran in a concentration-dependent manner, while we observed minimal binding to healthy PBMCs (Fig. 1b). The tested cancer cell lines were included due to their different epithelial phenotypes defined by the expression of two commonly used epithelial CTC markers, EpCAM and CK (Supplementary fig. 1b, c). Importantly, rVAR2 binding did not correlate to EpCAM nor the CK status of the cell lines.

The ofCS binding region of the large rVAR2 protein contains two conserved tryptophan residues in a WIW-motif flanked by multiple lysine-residues (<sup>555</sup>KKKWIWKK<sup>562</sup>)<sup>26</sup>. Substitution of the WIW-motif and the flanking lysine residues with alanine residues (rVAR2 mutant) induces a structural change of the chondroitin sulfate (CS) binding groove, resulting in decreased binding of rVAR2 to ofCS<sup>27</sup>. To determine if binding to the cancer cells was mediated by rVAR2 on the dextran polymer specifically, we compared the binding of mutant dextran-coupled rVAR2 to cancer cells with that of wildtype rVAR2:dextran. No binding of the mutant rVAR2 to any of the cancer cell lines was observed, validating the rVAR2-specific interaction (Fig. 1c, Supplementary fig. 1d). Next, we assessed the binding of rVAR2:dextran to cancer cells by flow cytometry after enzymatic digestion

**Fig. 2 | rVAR2:dextran stains cancer cells in blood.**

**a** Representative images of cancer cells (A549, ES-2 or COLO205) spiked into 1 mL of healthy donor blood followed by staining with rVAR2:dextran conjugated to PE (yellow), APC-conjugated antibodies targeting CD45/CD66b/CD16 (magenta) and DAPI (blue). Scale bar is 30  $\mu$ m. **b** Recovery (%) of 10, 50 or 100 cancer cells spiked into 1 mL of healthy donor blood. The samples were stained and identified as described in (a).

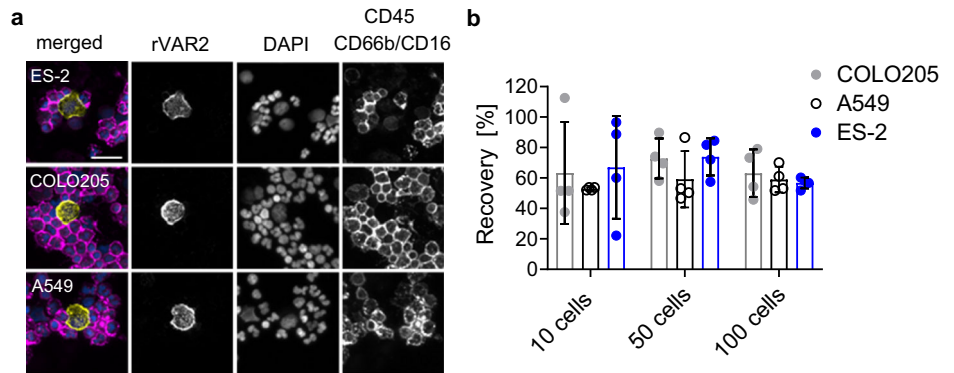
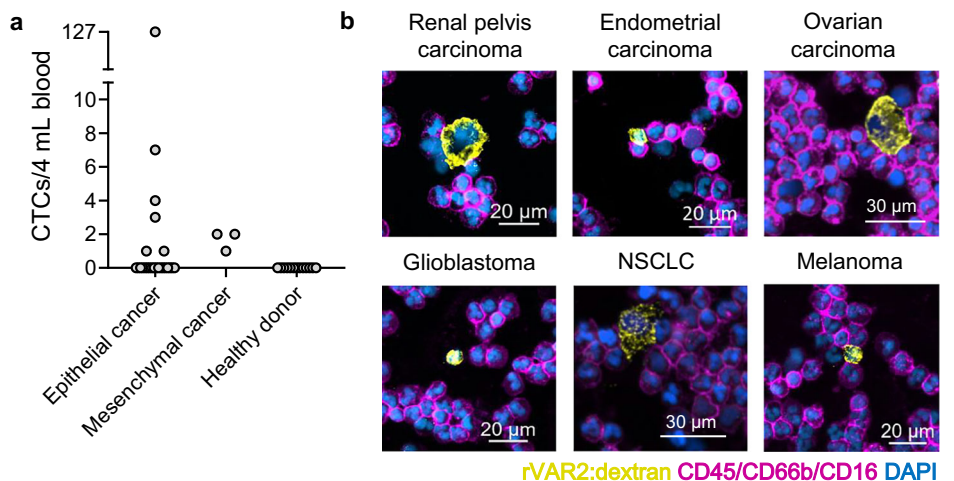


**Fig. 3 | Detection of ofCS + CTCs in patients with advanced cancer.**

**a** The number of ofCS+ CTCs detected with rVAR2:dextran in 4 mL of blood in patients with epithelial cancer (n = 25) or mesenchymal cancer (n = 3) and in healthy controls (n = 13). The samples were stained with PE-labelled rVAR2:dextran and APC-conjugated antibodies targeting CD45, CD66b and CD16. Cell nuclei were stained with DAPI. **b** Representative immunofluorescence images of ofCS+ CTCs from six different cancer patients. The CTCs were stained as described in (a). A CTC was defined as ofCS(+), CD45(–), CD66b(–), CD16(–) and DAPI(+).



of cell-surface CS chains using chondroitinase ABC as well as digestion of the similarly negatively charged heparan sulfate (HS) chains using heparinase. As expected, pre-digestion of HS had no effect on rVAR2:dextran binding to the cancer cells (Fig. 1d), whereas pre-digestion of CS completely abolished rVAR2:dextran binding (Fig. 1e, Supplementary fig. 1e). Furthermore, addition of soluble CS to the rVAR2:dextran staining mix inhibited binding to the cancer cells while addition of HS had little effect, again confirming the specificity to CS (Fig. 1f+ Supplementary fig. 2a, b).

### rVAR2:dextran detects cancer cells spiked into blood

To test if the rVAR2:dextran staining can specifically distinguish cancer cells from PBMCs, 10, 50, or 100 cancer cells were spiked into healthy donor blood. After spike in, the plasma fraction was removed by centrifugation followed by red blood cell lysis. Subsequently, the nucleated cells were incubated with a mix of the rVAR2:dextran complex and fluorophore-conjugated antibodies targeting leukocyte markers CD45, CD66b, and CD16. Following staining, the cells were fixed and stained with DAPI to detect cell nuclei. A cancer cell was defined as ofCS+, DAPI+, CD45–, CD66b– and CD16– as exemplified in Fig. 2a. The average cancer cell recovery was above 50%, demonstrating a reliable and efficient recovery. Importantly, the recovery was unaffected by the number of cancer cells spiked into the blood, indicating a high sensitivity for CTC detection (Fig. 2b).

### Clinical proof-of-concept of the rVAR2:dextran based method in patient samples

To evaluate the clinical applicability of the rVAR2-dextran staining for CTC detection, we tested the method in two independent cohorts: i) patients with

advanced cancer and ii) patients with suspected but undiagnosed cancer. These cohorts were selected as they represent multiple different cancer types as well as two different clinical settings, providing challenges highly relevant for cancer biomarker testing. Only ofCS+, DAPI+, CD45–, CD66b–, and CD16– cells were considered CTCs.

The cohort of patients with advanced cancer (n = 28) included eleven different cancer types of both epithelial and non-epithelial origin (Supplementary table 1). Six out of the 25 patients (24%) with carcinomas had detectable ofCS+ CTCs ranging from 1–127 cells per 4 mL of whole blood, while 3 out of 3 patients (100%) with non-epithelial cancers had 1 or 2 ofCS+ CTCs in the same blood volume (Fig. 3a). The distribution of CTC positive patients is shown in supplementary table 1. Notably, ofCS+ CTCs were detected across 7 out of the 11 cancer types, including patient groups in which the sensitivity of the established CTC strategies remains suboptimal such as non-small cell lung cancer, urothelial carcinoma, ovarian carcinoma, and glioblastoma<sup>28–35</sup>. Importantly, no ofCS+ cells were detected in blood samples from 13 healthy donors, highlighting the cancer specificity of the rVAR2:dextran staining (Fig. 3a, Supplementary table 1).

Besides being independent of tissue-origin, this ofCS staining method does not pre-select CTCs based on affinity purification or physical characteristics, which allows for the identification of CTCs with varying morphology. In the 9 patients with advanced cancer and detectable ofCS+ CTCs, we observed a high degree of heterogeneity in terms of cell shape and size (Fig. 3b). Furthermore, we detected ofCS+ CTCs with a range of different morphological appearances in a single patient diagnosed with metastatic high-grade serous ovarian carcinoma. Here, the ofCS+ CTCs could be grouped into four categories including (1) CTCs with a cell diameter greater than the adjacent blood cells (n = 52); (2) large and elongated

CTCs with defined cellular protrusions (n = 35); (3) CTC clusters of more than two cells (n = 5); and (4) small CTCs with an overlapping cell diameter compared to the adjacent blood cells (n = 35) (Fig. 4, Supplementary fig. 3).

We next applied the rVAR2:dextran method to a cohort of patients with serious non-specific symptoms or signs of cancer such as fatigue, weight loss, or diffuse pain, referred to an outpatient hospital clinic specialized in tailoring cancer diagnostic programs for such cases (n = 80, Supplementary fig. 4)<sup>36–38</sup>. This cohort represented a diverse population suffering from a spectrum of conditions, including various types of cancer, autoimmune diseases, or infections<sup>36,39</sup>. After completing the diagnostic program, 11 out of 80 patients (13.75%) were diagnosed with cancer, representing both hematologic cancer (n = 4) and malignant solid tumors (n = 7). Blood sample analysis showed detectable ofCS+ CTCs in 4 (57.1%) of the patients with solid colorectal or prostate tumors (Table 1). No obvious correlation was observed between ofCS positivity, cancer staging, or presence of metastasis (Supplementary table 2). Additionally, no specific

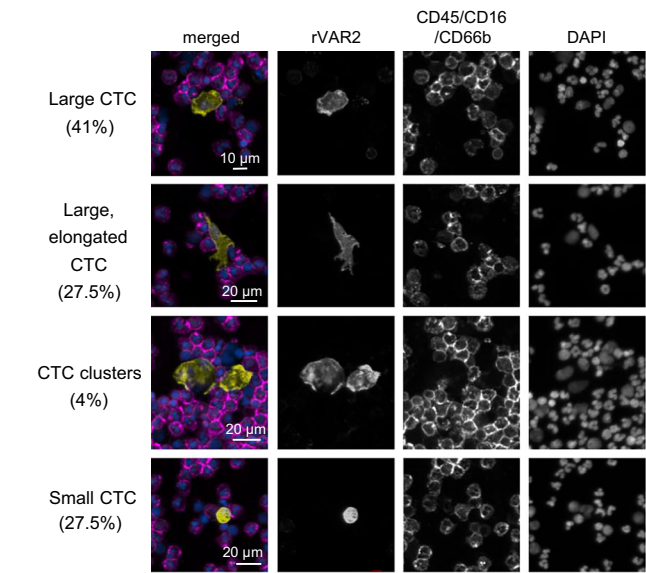


**Fig. 4 | Detection of morphologically diverse ofCS+ CTCs.** The figure shows four different morphological categories used to describe the ofCS+ CTCs detected in a blood sample from a patient with high-grade serous ovarian cancer. The sample was stained with rVAR2:dextran (yellow), CD45/CD16/CD66b (magenta) and DAPI (blue).

comorbidity or levels of standard cancer biomarkers (CEA, PSA, CA125, and CA19-9) was associated with the presence of ofCS+ CTCs (Supplementary table 2).

In hematological cancers, the tumor cells arise from the hematopoietic cell lineage and co-express leukocyte markers such as CD45, and therefore, we could not report them as CTCs in this study as we used CD45 positivity as one of our exclusion criteria. Still, 1 out of the 4 patients diagnosed with a hematologic cancer (multiple myeloma) had presence of 37 ofCS positive and CD45 negative CTCs in the blood sample (Table 1). This observation could potentially be explained by high phenotypic heterogeneity in multiple myeloma patients, in which reduction of CD45 on the cancer cells has been observed in late-stage patients<sup>40</sup>.

Interestingly, 6 out of the 69 patients (8.7%) who did not receive an initial cancer diagnosis had detectable ofCS+ CTCs (Table 2). Two patients had previously been diagnosed with either breast cancer or lymphoma, but no relapse was observed at the time of blood sampling. Furthermore, the plasma levels of standard cancer biomarkers (CEA, CA-125, CA19-9 and PSA) were within the normal range in all six patients (Supplementary Table 2).

Fifteen months after the initial investigations, the follow-up status was recorded in all patients who did not receive an initial cancer diagnosis. Here, 2 out of the 69 patients had a subsequent cancer; a neuroendocrine tumor in the ileum (8 months) and metastatic basosquamous carcinoma (15 months), respectively. No ofCS+ CTCs were detected in the patient with a neuroendocrine tumor, however, the patient with subsequent

| Table 2   Patients without confirmed cancer diagnosis but detectable ofCS+ cells |           |                               |                                  |
|--|-----------|-------------------------------|----------------------------------|
| Initial diagnosis  | # of CTCs | Previous cancer               | Cancer status after 15 months    |
| No cancer  | 1         | No cancer                     | Stage III basosquamous carcinoma |
| No cancer  | 4         | No cancer                     | No cancer                        |
| No cancer  | >1000     | No cancer                     | No cancer                        |
| No cancer  | 8         | No cancer                     | No cancer                        |
| No cancer  | 2         | Breast cancer                 | No cancer                        |
| No cancer  | 6         | Diffuse large B-cell lymphoma | No cancer                        |

Each row represents one individual patient from the DOC cohort. The number of ofCS+ CTCs is reported per 4 mL of whole blood.

**Table 1 | Patients with a confirmed cancer diagnosis in the DOC cohort**

| Cancer diagnosis              | Tumor classification |                       |                    | # of CTCs |
|-------------------------------|----------------------|-----------------------|--------------------|-----------|
|                               | Tumor stage          | Lymph node metastasis | Distant metastasis |           |
| Prostate                      | I                    | No                    | No                 | >1000     |
| Prostate                      | II                   | No                    | No                 | 0         |
| Prostate                      | II                   | No                    | No                 | 0         |
| Prostate                      | IV                   | Yes                   | Yes                | 1         |
| Colorectal (c.colon)          | IV                   | Yes                   | Yes                | 47        |
| Colorectal (c.rectum)         | III                  | Yes                   | No                 | 0         |
| Colorectal (c.cecum)          | IV                   | Yes                   | Yes                | 1         |
| Hodgkin's lymphoma            | 1 A/B                | —                     | —                  | NA        |
| Diffuse large B-cell lymphoma | 3 A/B                | —                     | —                  | NA        |
| Lymphoma                      | 4 A/B                | —                     | —                  | NA        |
| Multiple myeloma              | ISS2                 | —                     | —                  | 37        |

Each row represents individual patients. AJCC cancer staging was used for solid tumors (carcinomas), R-ISS staging was used for multiple myeloma, and Lugano staging was used for lymphomas. 4 mL of blood was used for CTC detection. NA non-applicable.



disseminated skin cancer had presence of ofCS+ CTCs in the blood sample at the first DOC visit (Table 2).

## Discussion

In this study, we present a platform-independent CTC detection strategy based on targeting the glycosaminoglycan structure, ofCS, uniquely modified in cancers and ubiquitously expressed on malignant cells. We show that the recombinant protein rVAR2 coupled to a fluorophore-labelled dextran detects cancer cells spiked into blood without the need for pre-enrichment, allowing for the specific identification of tumor cells with various epithelial phenotypes and morphologies. The dextran backbone has previously been used to detect and monitor specific T-cell clones by flow cytometry, however, to our knowledge, this is the first application of the strategy in rare CTC detection<sup>41,42</sup>.

With the advancements in algorithm-based image analysis and deep learning networks, the development of image-driven platforms for CTC analysis has emerged as a promising strategy. Several platforms, such as RareCyte<sup>TM</sup> and EPIC<sup>TM</sup> sciences, do not require pre-enrichment of the target cells and utilize high-throughput image-based data of immunofluorescence-stained cells for CTC analysis<sup>43–45</sup>. In particular, the EPIC<sup>TM</sup> platform has been widely used and analytically validated in metastatic prostate cancer patients, showing detection of a broad repertoire of prostate CTC subtypes using CK for cell identification<sup>43,46,47</sup>. While CK is commonly used for CTC detection in patients with epithelial cancers, it is not applicable for mesenchymal cancers. Additionally, CK expression can decrease in cells undergoing EMT. Therefore, new markers are needed to identify CTCs exhibiting mesenchymal phenotypes.

Several studies have established a link between CTCs that have undergone EMT and the acquisition of stem cell properties, leading to enhanced metastatic ability and acquired therapy resistance<sup>48–51</sup>. Notably, a recent study showed that rVAR2-captured CTCs from patients with pancreatic cancer include a subset of cancer stem cells<sup>24</sup>. In line with this, ofCS is continuously displayed on cancer cells during phenotype transition to a mesenchymal state *in vitro* after induction of EMT by TGF- $\beta$  treatment<sup>22,25</sup>. Similarly, in this study, rVAR2:dextran staining enabled the identification of ofCS+ CTCs with diverse phenotypes. One patient with metastatic ovarian cancer displayed CTC populations with varying morphologies, suggesting a high level of intra-tumoral heterogeneity. For instance, 27.5% of the observed ofCS+ CTCs were large and elongated with distinct cellular protrusions, indicating an invasive and mesenchymal-like phenotype. This finding is in accordance with a study reporting CTCs with mesenchymal features in metastatic ovarian cancer patients undergoing platinum-based chemotherapy<sup>52</sup>. Together, this indicates that rVAR2:dextran staining can be used to detect CTCs with different phenotypes. Thus, to investigate the ofCS expression on different CTC subpopulations further, additional antibodies targeting markers present on cancer stem cells, as well as markers present on epithelial and mesenchymal CTC phenotypes, would be valuable to include in the staining mix. Additionally, an in-depth molecular analysis of the CTCs would be needed to characterize the ofCS+ CTC population in more detail. Unfortunately, single-cell analysis was not possible in this study. It is probable that further optimization of the methodology, perhaps by combining the rVAR2:dextran staining with other CTC platforms that enable single-cell isolation, would allow a better characterization of these cells, ultimately providing a pathway to identify new therapeutic targets.

To show clinical proof-of-concept of targeting ofCS on CTCs in a broad range of cancer types, we applied the rVAR2-based detection to blood samples from a heterogeneous population of cancer patients with varying disease severity, different cancer diagnoses, and treatment histories. In the cohort of patients with diverse and advanced cancers, we found ofCS+ CTCs in 7 out of the 11 cancer types investigated, including both epithelial and non-epithelial cancers. Yet, for patients with epithelial cancer, only 24% of patients had ofCS+ CTCs. Due to the low number of patients in each subgroup, an expansion of the study with more patients is needed to draw conclusions on the assay sensitivity for individual cancer types. One potential explanation for the low detection rate in the clinical cohorts could

be the number of centrifugation steps during the staining protocol, potentially leading to cell loss. Despite the robust recovery observed when spiking cancer cell lines into whole blood, improvements in the assay design either through fewer centrifugations or by fixing the cells earlier in the process, might increase the detection of patient CTCs in the future. Another limitation of the study is the low volume of blood analyzed from each patient (4 mL) compared to other established CTC platforms that use 7.5 mL blood as a standard<sup>53,54</sup>. As CTCs are extremely rare, future studies utilizing larger blood volumes would be valuable to increase the detection rate, and directly compare the detection of ofCS+ CTCs using the rVAR2:dextran with other CTC platforms. Alternatively, staining with rVAR2:dextran downstream of diagnostic leukapheresis that enrich CTCs through continuous centrifugation of peripheral blood could be applied to increase the assay sensitivity and ofCS+ CTC detection<sup>55,56</sup>.

Prior to diagnosis, more than 25% of patients with cancer present with a broad range of nonspecific symptoms that cannot be related to a specific organ system<sup>36</sup>. This diversity in symptoms poses a challenge in devising an effective diagnostic approach, potentially resulting in diagnostic delay or false negative results where the patient is discharged from a diagnostic clinic without a confirmed cancer diagnosis, only to return shortly after with cancer<sup>39</sup>. Out of the 80 patients in the diagnostic outpatient clinic cohort, 13.8% were confirmed to have cancer. This distribution aligns with the reported cancer prevalence of prior national studies investigating patients referred to similar diagnostic clinics<sup>37–39</sup>. The rVAR2:dextran workflow detected ofCS+ CTCs in 57.1% of patients diagnosed with a solid tumor. However, a limitation of this study includes detection of CTCs in patients with hematological cancers. This shortfall is primarily explained by the fact that hematologic CTCs often co-express leukocyte markers, which hampers CTC detection in our assay. To adapt the rVAR2-based detection to include patients with hematological malignancies, alternative markers instead of CD45 are needed to distinguish non-malignant blood cells in the processing.

Among the 69 patients who did not receive an initial cancer diagnosis, we observed circulating ofCS+ CTCs in 6 patients. One of these patients was later diagnosed with metastatic skin cancer, indicating that these tumor cells could be circulating before the cancer became detectable in the clinic. Within the remaining 5 patients, 2 patients had previously been diagnosed with either lymphoma (11 years) or breast cancer (5 years) prior to referral to the diagnostic outpatient clinic. Emerging evidence suggests that residual cancer cells can remain dormant for years until subsequent outgrowth of metastasis, resulting in late disease recurrence in breast cancer patients<sup>57</sup>. Moreover, lymphoma survivors have an increased risk of developing secondary malignancies due to both intrinsic disease factors and the effects of previous chemotherapy and radiation treatments<sup>58,59</sup>. For instance, a retrospective study of 142,637 patients diagnosed with Non-Hodgkin's lymphoma found that 11.3% of the patients later developed secondary malignancies with breast, head, and neck and bladder cancer being the most prevalent cancer types after 10 years<sup>60</sup>. Whether the presence of ofCS+ CTCs in the blood serves as an indicator of disease recurrence or the development of a secondary malignancy remains to be determined. However, a recent UK study found that among the patients participating in an urgent cancer referral program who did not receive an initial cancer diagnosis, 1,338 per 100,000 were later diagnosed with cancer within 5 years<sup>61</sup>. This frequency was higher than the background population, which could indicate that the follow-up period of 15 months in this study might have been too short to determine whether the detected ofCS positive cells in the undiagnosed patients ( $n = 5$ ) were false-positive events or indicators of an occult tumor.

In conclusion, targeting of ofCS on CTCs using the rVAR2 protein coupled to a dextran backbone provides a method for multi-cancer and platform independent CTC detection in patients with diverse cancers. In the future, the ofCS staining strategy could potentially be implemented as a staining mix in other CTC platforms, offering enhanced detection of non-epithelial and mesenchymal-like CTCs. Furthermore, as the ofCS-modification is present at the cell surface, this strategy could also enable the identification of live CTCs for *ex vivo* culturing or transcriptomic

profiling, bypassing the need for cell fixation and intracellular staining known to affect RNA integrity.

## Methods

### Patient sample collection and eligibility

Two clinical centers participated in this study: (a) The Phase I Unit at the Department of Oncology, Copenhagen University Hospital—Rigshospitalet, Denmark, and (b) the Diagnostic Outpatient Clinic (DOC), Copenhagen University Hospital—Herlev and Gentofte, Denmark.

Peripheral blood samples were collected in K<sub>2</sub>EDTA tubes (BD Biosciences), and 4 mL was used for CTC analysis. The blood samples were processed within two hours of collection at the Center for Translational Medicine and Parasitology at University of Copenhagen, Denmark.

Collection of blood samples from healthy asymptomatic control subjects ( $n = 13$ ) who had no history of malignant disease and no known illness at the time of blood collection was approved by the Danish Regional Ethics Committee (H-19039400). The study was conducted in compliance with the principles of the Declaration of Helsinki, and all the enrolled patients and healthy subjects gave written informed consent before inclusion according to the guidelines of the Danish Ethics Committee.

### Phase I cohort

From September 2020 to February 2023, 28 patients with advanced solid cancers were eligible for the study as part of the Copenhagen Prospective Personalized Oncology study (CoPPO, NCT02290522). The study was approved by the Danish Data Protection Agency (j.no.: 2012-58-004) and the Regional and National Ethics Committees (file number: 1300530 and H-16046103, respectively)<sup>62</sup>. Testing of new experimental cancer treatments is often conducted in this clinical setting, in which implementation of new liquid biomarkers might be of value to evaluate both the clinical and therapeutic benefit of a given drug<sup>63</sup>. In this study, all patients had previously exhausted every standard treatment options and were referred to the Phase I Unit for experimental treatment<sup>62</sup>. The blood sample for CTC analysis was collected before initiation of treatment.

### DOC cohort

From December 2021 to April 2023, 87 patients were enrolled in this study under the MICA protocol approved by the Danish Regional Ethics Committee (H-7-2014-011), investigating translational biomarkers of early cancer diagnosis. Seven patients were excluded from the study population, of which five were based on deviations in sample processing. In addition, one patient was excluded upon discovery of concurrent treatment for a previously diagnosed cancer at the time of inclusion, and one patient passed away before the diagnostic investigation was completed (Supplementary Fig. 4). The criteria for referral to the DOC have been described in more detail elsewhere<sup>37</sup>. Briefly, all patients donated blood before a final diagnosis was made. During the diagnostic evaluation, the patients underwent a series of diagnostic investigations, including a battery of blood tests with standard or explorative biomarkers, diagnostic imaging, and tissue biopsies when indicated. When a specific disease or type of cancer was diagnosed or suspected, the patient was referred to an organ-specific cancer patient pathway or other medical specialists<sup>37,39,64</sup>. Cancer-specific mortality, emigration, or death due to other causes were recorded, and follow-up cancer diagnosis was available after 15 months of DOC inclusion by reviewing of electronic medical records.

### Protein production

The recombinant truncated VAR2CSA protein (rVAR2) spanning the DBL1-ID2a domains and the non-ofCS binding rVAR2 mutant DBL1-ID2a<sup>555</sup>AAAAIAAA<sup>562</sup> including a His tag, Spytag, and C-terminal V5-tag was expressed in Shuffle T7 Express Competent *E. coli* cells (New England Biolabs, C3029J)<sup>27</sup>. Following lysis of the cell pellet, the soluble rVAR2 protein was purified using two chromatography steps. Firstly, an affinity step using HisTrap HP (Cytiva, USA) and secondly, a cation exchange step HiTrap SP HP (Cytiva, USA), as previously described<sup>16</sup>. The purity of the

monomeric proteins was analyzed by SDS-PAGE, and the specificity towards ofCS was ensured by ELISA and flow cytometry, as previously described<sup>23,25</sup>. The SpyCatcher protein with a C-terminal 6x-histidine tag was produced in *E. coli* BL21 DE3 cells (C2527H, New England Biolabs). The SpyCatcher domain with histidine tag was purified using affinity chromatography using a HisTrap HP column (Cytiva) followed by anion exchange chromatography using HiTrap Q HP column (Cytiva). Subsequently, the SpyCatcher was biotinylated using NHS-biotin (Sigma-Aldrich) dissolved in DMSO. The NHS-biotin was mixed with SpyCatcher in a 10:1 molar ratio. After 1 h of incubation (room temperature), the biotinylated SpyCatcher proteins were purified using a Zeba™ spin column with 7 kDa cutoff (Thermo Fischer). The purity of the protein and its ability to form an isopeptide bond to Spy-tagged rVAR2 was evaluated by SDS-Page. The Chondroitinase ABC (Uniprot P59807) protein with a C-terminal 6x-histidine tag was expressed in *E. coli* Shuffle T7 express (C3029J, New England Biolabs). The protein was purified using two chromatography steps, first an affinity step on HisTrap HP (Cytiva) and subsequently size exclusion using Sephacryl S-300 (Cytiva).

### Conjugation of rVAR2 to fluorophore-labelled dextran

The rVAR2 protein was biotinylated through the SpyTag-SpyCatcher technology by mixing of SpyTagged-rVAR2 with biotinylated SpyCatcher in a 1.2:1 molar ratio. The mixed proteins were incubated for 1 hour at room temperature. Next, the biotinylated rVAR2 proteins were coupled to a dextran backbone carrying both PE fluorophores and streptavidin (DX01-PE, Immudex, Denmark). The PE-labelled dextran backbone contained 5 streptavidin molecules equal to 20 biotin-acceptor sites. For conjugation of biotinylated rVAR2 to the dextran, rVAR2 and dextran were mixed in a 15:1 molar ratio to occupy ~75% of the biotin acceptor sites. The mix was incubated, protected from light, for 30 min at room temperature and stored on ice until use for maximum 30 min. The conjugation volume was calculated according to the manufacturer's recommendation (Immudex, Denmark).

### Cell culturing

The A549 and COLO205 cell lines originated from the American Type Culture Collection (ATCC). The ES-2 cells were kindly gifted from Mads Daugaard (University of British Columbia, Canada). The A549 cell line was cultured in DMEM GlutaMax (Gibco®, 10566-016). The COLO205 cell line was maintained in RPMI 1640 (Gibco®, 61870-010), and the ES-2 cell line was cultured in McCoy's 5a medium (Sigma, M9309) with an additional supplement of 1% L-Glutamine (Merck, G7513). All cell media were supplemented with 10% fetal bovine serum (FBS, Thermo Fischer, 10270-106) and 1% penicillin-streptomycin (Pen/Strep, Gibco® Life Technologies). The cells were maintained at 37 °C, 5% CO<sub>2</sub>, and passaged when reaching ~70% confluence. Cell cultures were tested for mycoplasma contamination on a regular basis, and all experiments were performed with mycoplasma-free cells.

### Staining specificity testing

Cancer cells grown at ~70% confluence were detached using Accutase (Gibco®, A111-05-01) and washed using Dulbecco's PBS (DPBS, Sigma, D8537) containing 2% FBS (Thermo Fischer, 10270-106). In some experiments, a portion of the cancer cells were pre-treated with chondroitinase ABC (chABC, 20 µg/mL) or a heparinase (HSase) mix (2.5 mU/mL HSase II + 5 mU/mL HSase III, IBEX) in DPBS containing 2% FBS for 30 min (37 °C). As a control, untreated cells were incubated for 30 min (37 °C) in DPBS containing 2% FBS. The cells were washed twice in DPBS containing 2% FBS and placed into a 96-well round-bottom plate or a 1.5 mL Eppendorf tube at 10<sup>5</sup> cells per well/tube, depending on the setup. Next, the cells were incubated for 30 min (4 °C) with either 3 nM (flow cytometry read-out) or 4 nM (fluorescence microscopy read-out) of PE-labelled rVAR2:dextran in DPBS containing 2% FBS with an adjusted NaCl concentration of 300 mM. For inhibition assays, 25 µg/mL of soluble CS (amsbio, 370710-IEC) or 25 µg/mL of soluble HS (Sigma, H7640) were

added to the rVAR2:dextran staining mix. To measure the efficiency of the HSase enzyme treatment, the cancer cells were incubated with a primary anti-HS antibody (amsbio, 370255-S, 1:1000) in DPBS containing 2% FBS for 30 min. (4 °C). The cells were then washed twice and incubated with a FITC-conjugated goat anti-Mouse IgM secondary antibody in DPBS containing 2% FBS for 30 min. (Invitrogen, cat. no. 31992, 1:100) see Supplementary Fig. 1a.

Next, the cells were washed twice in DPBS containing 2% FBS and fixed in 4% paraformaldehyde (PFA, Alfa Aesar, J61899.AK) for 5 min. at room temperature. For all flow cytometry experiments, the cells were diluted in DPBS and analyzed on the Cytotflex S instrument (Beckman-Coulter) including three technical replicates. Data analysis was performed using FlowJo software (v. 10.1). For fluorescence microscopy analysis, the cells were washed in DPBS after fixation, and the cell nucleus was stained with 4',6-diamidino-2-phenylindole (DAPI, 1:1000, Fischer Scientific, D1306) diluted in DPBS. Next, the cells were plated on a glass microscopy slide, mounted, and scanned using the Cytation™ 5 Cell Imaging Multi-Mode Reader (BioTek, 20× magnification, 0.8 N.A). The mean fluorescence intensities of the rVAR2:dextran-PE per cell were measured on 500 single cells from each condition in the Gen 5 software (version 3.10) using the analysis tool with a threshold value of 4000 (DAPI channel), min. object size of 5 µm and max object size of 100 µm.

### Epithelial marker analysis

Cancer cells at ~70% confluence were detached using Accutase and washed using DPBS containing 2% FBS. The cells were added to a 96-well round-bottom plate at 10<sup>5</sup> cells per well. For EpCAM detection, the cells were incubated with PE-conjugated anti-EpCAM (clone VU-1D9, Abcam, ab112068, 1:100) diluted in DPBS containing 2% FBS for 30 min. (4 °C). The cells were washed twice in DPBS containing 2% FBS and fixed with 4% PFA for 5 min. (room temperature) before flow cytometry analysis as previously described.

For analysis of CK expression, the cells were added to a 96-well round-bottom plate at 10<sup>5</sup> cells per well. The cells were washed in DPBS containing 2% FBS and fixed in 4% PFA for 5 min. (room temperature). The cells were washed twice in DPBS and permeabilized for 20 min. in DPBS containing 1% BSA (Sigma-Aldrich, A3059) and 0.15% Saponin (Sigma-Aldrich, 47036). Next, the cells were incubated for 30 min. with a cocktail of PE-conjugated CK antibodies (clone C-11, Abcam, ab52460, 1:50 and clone CK-19, Santa Cruz Biotechnology, sc-6278, 1:100) in DPBS containing 1% BSA and 0.05% Saponin. The cells were washed twice in DPBS and analyzed by flow cytometry as previously described.

### Cancer cells spiked into whole blood

Cancer cells at ~70% confluence were detached using Accutase and washed in DPBS. The cells were resuspended in 2 mL of pre-heated cell media, and the cell concentration was counted manually using a hemacytometer. For spiking of 100 cells, the cells were diluted to a concentration of 10,000 cells/mL in DPBS. A volume of 10 µL from the cell dilution was added to 1 mL of healthy donor blood. To estimate the number of cells spiked into the blood, 10 µL of the same cell dilution used for spiking was transferred to a microscopy slide (in triplicates), and the exact number of cells was manually counted using a light microscope (10× objective). The average cell count was set as a reference for calculating the percentage of recovered cells. For spike in of lower cell numbers, the cells were diluted to 5000 cells/mL (spike in of 50 cells) or 1000 cells/mL (spike in of 10 cells).

### Staining of CTCs in blood

After spiking of the cancer cells into whole blood, the plasma fraction was removed after centrifugation (400 x g, 10 min. at room temperature), and replaced with an equal volume of room-temperature DPBS containing 2% FBS. The red blood cells were subsequently lysed by diluting the sample in RBC lysis buffer, reaching a final concentration of 0.01 M potassium hydrogen carbonate, 0.155 M ammonium chloride, and 0.1 mM EDTA. After incubation for 13 min., the samples were centrifuged (400 x g, 8 min.

at room temperature), and the pelleted cells were washed in DPBS containing 2% FBS. Subsequently, the samples were stained with a cocktail of PE-conjugated dextran complexed with rVAR2 (4 nM) in combination with APC-labelled antibodies targeting CD45 (1:20, Thermo Fischer, 17-0459-42, clone: HI30), CD16 (1:40, Thermo Fischer, MHCD1605, clone: 3G8), and CD66b (1:20, Miltenyi Biotec, 130-117-692, clone: REA306) in DPBS containing 2% FBS with an adjusted NaCl concentration of 300 mM (final concentration). Following staining, the samples were washed in DPBS containing 2% FBS and fixed with cold 4% PFA for 5 min. Subsequently, the cell nuclei were stained with DAPI (1:1000) diluted in DPBS. The samples were plated on glass microscopy slides (1.5 × 10<sup>6</sup> cells per slide) and analyzed by fluorescence microscopy as described below.

### CTC identification

The samples were scanned using the Cytation™ 5 Cell Imaging Multi-Mode Reader (BioTek, 20× magnification, 0.8 N.A) or the Zeiss Axio Z1 automated slide scanner (20× magnification, 0.8 NA objective). The CTCs were enumerated manually using the Gen5 software (BioTek, version 3.10) or the Zeiss Zen Blue version 3.1 software. A CTC was defined based on ofCS(+) and DAPI(+), CD45(−), CD16(−), CD66b(−).

### Graphs and statistics

Figures were generated in Biorender, and all graphs and statistical analysis were generated using GraphPad Prism (v. 10.0.3). Data is presented as mean ± standard deviation. For comparison between groups, a one-way ANOVA test was used. The testing level  $\alpha = 0.05$  was used for all statistics.

### Data availability

The processed data that support the findings of this study are available within the article and its supplementary material. Due to privacy laws, the access and public availability of the raw image data files are restricted. The raw data can only be made available following approval from the data protection agencies in Denmark and the ethics committees. Request for access should be directed to the corresponding author.

### Abbreviations

|       |                                       |
|-------|---------------------------------------|
| CEA   | Carcinoembryonic antigen              |
| CK    | Cytokeratin                           |
| CS    | Chondroitin sulfate                   |
| CTC   | Circulating tumor cell                |
| DOC   | Diagnostic outpatient clinic          |
| EMT   | Epithelial-to-mesenchymal transition  |
| EpCAM | Epithelial cellular adhesion molecule |
| HS    | Heparan sulfate                       |
| NSCLC | Non-small cell lung cancer            |
| ofCS  | Oncofetal chondroitin sulfate         |
| PBMC  | Peripheral blood mononuclear cells    |
| rVAR2 | Recombinant VAR2CSA                   |

Received: 17 January 2025; Accepted: 5 May 2025;

Published online: 16 May 2025

### References

1. Alix-Panabieres, C. & Pantel, K. Liquid biopsy: from discovery to clinical application. *Cancer Discov.* **11**, 858–873 (2021).
2. Ring, A., Nguyen-Strauli, B. D., Wicki, A. & Aceto, N. Biology, vulnerabilities and clinical applications of circulating tumour cells. *Nat. Rev. Cancer* **23**, 95–111 (2023).
3. Vasseur, A., Kiavue, N., Bidard, F. C., Pierga, J. Y. & Cabel, L. Clinical utility of circulating tumor cells: an update. *Mol. Oncol.* **15**, 1647–1666 (2021).
4. Ignatiadis, M., Sledge, G. W. & Jeffrey, S. S. Liquid biopsy enters the clinic - implementation issues and future challenges. *Nat. Rev. Clin. Oncol.* **18**, 297–312 (2021).



5. Rushton, A. J., Nteliopoulos, G., Shaw, J. A. & Coombes, R. C. A Review of circulating tumour cell enrichment technologies. *Cancers (Basel)* **13**, <https://doi.org/10.3390/cancers13050970> (2021).
6. Keller, L., Werner, S. & Pantel, K. Biology and clinical relevance of EpCAM. *Cell Stress* **3**, 165–180 (2019).
7. Barak, V., Goike, H., Panaretakis, K. W. & Einarsson, R. Clinical utility of cytokeratins as tumor markers. *Clin. Biochem* **37**, 529–540 (2004).
8. Franken, A. et al. Comparative analysis of EpCAM high-expressing and low-expressing circulating tumour cells with regard to their clonal relationship and clinical value. *Br. J. Cancer* **128**, 1742–1752 (2023).
9. Mentink, A., Isebia, K. T., Kraan, J., Terstappen, L. & Stevens, M. Measuring antigen expression of cancer cell lines and circulating tumour cells. *Sci. Rep.* **13**, 6051 (2023).
10. Seo, J. et al. Plasticity of circulating tumor cells in small cell lung cancer. *Sci. Rep.* **13**, 11775 (2023).
11. Drucker, A., et al. Comparative performance of different methods for circulating tumor cell enrichment in metastatic breast cancer patients. *PLoS ONE* **15**, e0237308 (2020).
12. Miller, M. C., Robinson, P. S., Wagner, C. & O'Shannessy, D. J. The Parsortix Cell Separation System-A versatile liquid biopsy platform. *Cytom. A* **93**, 1234–1239 (2018).
13. West, R. C., Bouma, G. J. & Winger, Q. A. Shifting perspectives from “oncogenic” to oncofetal proteins; how these factors drive placental development. *Reprod. Biol. Endocrinol.* **16**, 101 (2018).
14. Ma, Y. et al. The relationship between early embryo development and tumorigenesis. *J. Cell Mol. Med* **14**, 2697–2701 (2010).
15. Sharma, A., Bleriot, C., Currenti, J. & Ginhoux, F. Oncofetal reprogramming in tumour development and progression. *Nat. Rev. Cancer* **22**, 593–602 (2022).
16. Salanti, A. et al. Targeting human cancer by a glycosaminoglycan binding malaria protein. *Cancer Cell* **28**, 500–514 (2015).
17. Dawood, Z. S. et al. Colonoscopy, imaging, and carcinoembryonic antigen: Comparison of guideline adherence to surveillance strategies in patients who underwent resection of colorectal cancer - A systematic review and meta-analysis. *Surg. Oncol.* **47**, 101910 (2023).
18. Galle, P. R. et al. Biology and significance of alpha-fetoprotein in hepatocellular carcinoma. *Liver Int.* **39**, 2214–2229 (2019).
19. Vidal-Calvo, E. E. et al. Tumor-agnostic cancer therapy using antibodies targeting oncofetal chondroitin sulfate. *Nat. Commun.* **15**, 7553 (2024).
20. Soares da Costa, D., Reis, R. L. & Pashkuleva, I. Sulfation of glycosaminoglycans and its implications in human health and disorders. *Annu Rev. Biomed. Eng.* **19**, 1–26 (2017).
21. Noborn, F., Nilsson, J. & Larson, G. Site-specific glycosylation of proteoglycans: a revisited frontier in proteoglycan research. *Matrix Biol.* **111**, 289–306 (2022).
22. Agerbaek, M. O. et al. The VAR2CSA malaria protein efficiently retrieves circulating tumor cells in an EpCAM-independent manner. *Nat. Commun.* **9**, 3279 (2018).
23. Sand, N. T. et al. Optimization of rVAR2-based isolation of cancer cells in blood for building a robust assay for clinical detection of circulating tumor cells. *Int. J. Mol. Sci.* **21**, <https://doi.org/10.3390/ijms21072401> (2021).
24. Tang, J. et al. CTC-derived pancreatic cancer models serve as research tools and are suitable for precision medicine approaches. *Cell Rep. Med.* **5**, 101692 (2024).
25. Bang-Christensen, S. R. et al. Capture and Detection of Circulating Glioma Cells Using the Recombinant VAR2CSA Malaria Protein. *Cells* **8**, <https://doi.org/10.3390/cells8090998> (2021).
26. Ma, R. et al. Structural basis for placental malaria mediated by Plasmodium falciparum VAR2CSA. *Nat. Microbiol.* **6**, 380–391 (2021).
27. Wang, K. et al. Cryo-EM reveals the architecture of placental malaria VAR2CSA and provides molecular insight into chondroitin sulfate binding. *Nat. Commun.* **12**, 2956 (2021).
28. Andrikou, K. et al. Circulating tumour cells: detection and application in advanced non-small cell lung cancer. *Int. J. Mol. Sci.* **24**, <https://doi.org/10.3390/ijms242216085> (2023).
29. Obermayr, E. et al. Circulating tumor cells: potential markers of minimal residual disease in ovarian cancer? a study of the OVCAD consortium. *Oncotarget* **8**, 106415–106428 (2017).
30. Gallagher, D. J. et al. Detection of circulating tumor cells in patients with urothelial cancer. *Ann. Oncol.* **20**, 305–308 (2009).
31. Riethdorf, S., Soave, A. & Rink, M. The current status and clinical value of circulating tumor cells and circulating cell-free tumor DNA in bladder cancer. *Transl. Androl. Urol.* **6**, 1090–1110 (2017).
32. Tamminga, M. et al. Leukapheresis increases circulating tumour cell yield in non-small cell lung cancer, counts related to tumour response and survival. *Br. J. Cancer* **126**, 409–418 (2022).
33. Asante, D. B., Calapre, L., Ziman, M., Meniawy, T. M. & Gray, E. S. Liquid biopsy in ovarian cancer using circulating tumor DNA and cells: ready for prime time?. *Cancer Lett.* **468**, 59–71 (2020).
34. Westphal, M. et al. Circulating tumor cells and extracellular vesicles as liquid biopsy markers in neuro-oncology: prospects and limitations. *Neurooncol. Adv.* **4**, ii45–ii52 (2022).
35. Papadaki, M. A. et al. Assessment of the efficacy and clinical utility of different circulating tumor cell (CTC) detection assays in patients with chemotherapy-naïve advanced or metastatic non-small cell lung cancer (NSCLC). *Int. J. Mol. Sci.* **22**, <https://doi.org/10.3390/ijms22020925> (2021).
36. Gronnemoose, R. B. et al. Risk of cancer and serious disease in Danish patients with urgent referral for serious non-specific symptoms and signs of cancer in Funen 2014–2021. *Br. J. Cancer* **130**, 1304–1315 (2024).
37. Videmark, A. N. et al. Combined plasma C-reactive protein, interleukin and YKL-40 for detection of cancer and prognosis in patients with serious nonspecific symptoms and signs of cancer. *Cancer Med.* **12**, 6675–6688 (2023).
38. Ingeman, M. L., Christensen, M. B., Bro, F., Knudsen, S. T. & Vedsted, P. The Danish cancer pathway for patients with serious non-specific symptoms and signs of cancer-a cross-sectional study of patient characteristics and cancer probability. *BMC Cancer* **15**, 421 (2015).
39. Moseholm, E. & Lindhardt, B. O. Patient characteristics and cancer prevalence in the Danish cancer patient pathway for patients with serious non-specific symptoms and signs of cancer-A nationwide, population-based cohort study. *Cancer Epidemiol.* **50**, 166–172 (2017).
40. Kumar, S., Rajkumar, S. V., Kimlinger, T., Greipp, P. R. & Witzig, T. E. CD45 expression by bone marrow plasma cells in multiple myeloma: clinical and biological correlations. *Leukemia* **19**, 1466–1470 (2005).
41. Saini, S. K. et al. Neoantigen reactive T cells correlate with the low mutational burden in hematological malignancies. *Leukemia* **36**, 2734–2738 (2022).
42. Mold, J. E. et al. Divergent clonal differentiation trajectories establish CD8(+) memory T cell heterogeneity during acute viral infections in humans. *Cell Rep.* **35**, 109174 (2021).
43. Werner, S. L. et al. Analytical validation and capabilities of the epic CTC platform: enrichment-free circulating tumour cell detection and characterization. *J. Circ. Biomark.* **4**, 3 (2015).
44. Scher, H. I. et al. Development and validation of circulating tumour cell enumeration (Epic Sciences) as a prognostic biomarker in men with metastatic castration-resistant prostate cancer. *Eur. J. Cancer* **150**, 83–94 (2021).
45. Yeo, D. et al. Accurate isolation and detection of circulating tumor cells using enrichment-free multiparametric high resolution imaging. *Front Oncol.* **13**, 1141228 (2023).
46. McDaniel, A. S. et al. Phenotypic diversity of circulating tumour cells in patients with metastatic castration-resistant prostate cancer. *BJU Int.* **120**, E30–E44 (2017).
47. Malihi, P. D. et al. Single-cell circulating tumor cell analysis reveals genomic instability as a distinctive feature of aggressive prostate cancer. *Clin. Cancer Res.* **26**, 4143–4153 (2020).



48. Aiello, N. M. et al. EMT subtype influences epithelial plasticity and mode of cell migration. *Dev. Cell* **45**, 681–695.e684 (2018).
49. Tsao, S. C. et al. Characterising the phenotypic evolution of circulating tumour cells during treatment. *Nat. Commun.* **9**, 1482 (2018).
50. Sun, Y. F. et al. Circulating tumor cells from different vascular sites exhibit spatial heterogeneity in epithelial and mesenchymal composition and distinct clinical significance in hepatocellular carcinoma. *Clin. Cancer Res.* **24**, 547–559 (2018).
51. Patel, S., Shah, K., Mirza, S., Shah, K. & Rawal, R. Circulating tumor stem like cells in oral squamous cell carcinoma: an unresolved paradox. *Oral. Oncol.* **62**, 139–146 (2016).
52. Chebouti, I. et al. EMT-like circulating tumor cells in ovarian cancer patients are enriched by platinum-based chemotherapy. *Oncotarget* **8**, 48820–48831 (2017).
53. Riethdorf, S. et al. Detection of circulating tumor cells in peripheral blood of patients with metastatic breast cancer: a validation study of the CellSearch system. *Clin. Cancer Res.* **13**, 920–928 (2007).
54. Riethdorf, S., O’Flaherty, L., Hille, C. & Pantel, K. Clinical applications of the CellSearch platform in cancer patients. *Adv. Drug Deliv. Rev.* **125**, 102–121 (2018).
55. Stoecklein, N. H., Fischer, J. C., Niederacher, D. & Terstappen, L. W. Challenges for CTC-based liquid biopsies: low CTC frequency and diagnostic leukapheresis as a potential solution. *Expert Rev. Mol. Diagn.* **16**, 147–164 (2016).
56. Rieckmann, L. M. et al. Diagnostic leukapheresis reveals distinct phenotypes of NSCLC circulating tumor cells. *Mol. Cancer* **23**, 93 (2024).
57. Klein, C. A. Cancer progression and the invisible phase of metastatic colonization. *Nat. Rev. Cancer* **20**, 681–694 (2020).
58. Sacchi, S. et al. Secondary malignancies after treatment for indolent non-Hodgkin’s lymphoma: a 16-year follow-up study. *Haematologica* **93**, 398–404 (2008).
59. Tarella, C. et al. Risk factors for the development of secondary malignancy after high-dose chemotherapy and autograft, with or without rituximab: a 20-year retrospective follow-up study in patients with lymphoma. *J. Clin. Oncol.* **29**, 814–824 (2011).
60. Parsons, M. W. et al. Secondary malignancies in non-Hodgkin lymphoma survivors: 40 years of follow-up assessed by treatment modality. *Cancer Med.* **12**, 2624–2636 (2023).
61. Scott, S. E. et al. Future cancer risk after urgent suspected cancer referral in England when cancer is not found: a national cohort study. *Lancet Oncol.* **24**, 1242–1251 (2023).
62. Tuxen, I. V. et al. Copenhagen Prospective Personalized Oncology (CoPPO)–Clinical Utility of Using Molecular Profiling to Select Patients to Phase I Trials. *Clin. Cancer Res.* **25**, 1239–1247 (2019).
63. Adashek, J. J., LoRusso, P. M., Hong, D. S. & Kurzrock, R. Phase I trials as valid therapeutic options for patients with cancer. *Nat. Rev. Clin. Oncol.* **16**, 773–778 (2019).
64. Vedsted, P. & Olesen, F. A differentiated approach to referrals from general practice to support early cancer diagnosis - the Danish three-legged strategy. *Br. J. Cancer* **112**, S65–S69 (2015).

## Acknowledgements

We would like to thank Sofie S. Espensen, Envy L. Masola, Muhammad T. Mukhtar, and Felix Fischer for their great work and technical assistance on the project. We would also like to acknowledge all the patients who participated in the study and give special thanks to Laurine Harsløf, Martin Højgaard, Iben Spanggaard, and the rest of the personnel at the Department of Oncology, Copenhagen University Hospital, Rigshospitalet, Denmark, together with Julia S. Johansen, Claus L. Feltøft, Mette K. Pedersen, Gitte Marianne Davidsen, and the rest of the personnel at the Department of Medicine, Copenhagen

University Hospital –Herlev and Gentofte, Denmark. We would also like to thank professor Mads Daugaard, University of British Columbia, Vancouver, Canada, for kindly providing the ES-2 cell line. Lastly, we would like to thank the Core Facility for Integrated Microscopy, Faculty of Health and Medical Sciences, University of Copenhagen, and the Core Facility for Flow Cytometry and Single Cell Analysis, Faculty of Health and Medical Sciences, University of Copenhagen, for their eminent technical assistance on the project. This study was funded by Innovation Fund Denmark (Grand Solutions, grant no 9090-00024B) and Novo Nordisk Foundation (Grant IDs: NNF19OC0058387, NNF21OC0068192, NNF22OC0076055). The funder played no role in study design, data collection, analysis and interpretation of data, or the writing of this manuscript.

## Author contributions

The work reported in the paper has been performed by the authors unless clearly specified in the text. Conceptualization, C.L., K.S.R., R.U., A.S., and M.Ø.A.; Acquisition of data and key reagents, C.L., C.F.S., K.S.R., N.T.S., J.M., T.G., and R.D.; Formal analysis, C.L.; Funding acquisition, K.S.R., R.U., T.G.T., A.S., and M.Ø.A.; Methodology C.L. and M.Ø.A.; Project administration, C.L., C.F.S., R.U., K.S.R., and M.Ø.A.; Visualization, C.L.; Writing—original draft, C.L. All authors reviewed the manuscript.

## Competing interests

The technology to diagnose cancer through rVAR2 is owned by VarCT Diagnostics through a license from VAR2Pharmaceuticals. A.S., M.Ø.A., and T.G.T. are cofounders of VAR2Pharmaceuticals. The remaining authors declare no competing interests.

## Additional information

**Supplementary information** The online version contains supplementary material available at <https://doi.org/10.1038/s41698-025-00936-3>.

**Correspondence** and requests for materials should be addressed to Mette Ø. Agerbæk.

**Reprints and permissions information** is available at <http://www.nature.com/reprints>

**Publisher’s note** Springer Nature remains neutral with regard to jurisdictional claims in published maps and institutional affiliations.

**Open Access** This article is licensed under a Creative Commons Attribution-NonCommercial-NoDerivatives 4.0 International License, which permits any non-commercial use, sharing, distribution and reproduction in any medium or format, as long as you give appropriate credit to the original author(s) and the source, provide a link to the Creative Commons licence, and indicate if you modified the licensed material. You do not have permission under this licence to share adapted material derived from this article or parts of it. The images or other third party material in this article are included in the article’s Creative Commons licence, unless indicated otherwise in a credit line to the material. If material is not included in the article’s Creative Commons licence and your intended use is not permitted by statutory regulation or exceeds the permitted use, you will need to obtain permission directly from the copyright holder. To view a copy of this licence, visit <http://creativecommons.org/licenses/by-nc-nd/4.0/>.

© The Author(s) 2025